School of Electrical Engineering and Telecommunications

Frequency Estimation for Three-Phase Power Systems

by

Shafee M Khalil

Thesis submitted as a requirement for the degree

Bachelor of Engineering (Electrical Engineering)

Supervisor: Dr. Elias Aboutanios   Student ID: z3318438
Assessor: Prof. David Taubman   Submission Date: October 30, 2014

Thesis title: Frequency Estimation for Three-Phase Power Systems
Topic number: EAB22

Student Name: Shafee M Khalil   **Student ID: z3318438**

A.   Problem statement

Estimation of a three-phase AC power system's operating frequency provides a reflection on power quality and system health. The difficulty in acquiring such an estimate from each individual phase voltages (as well as line-to-line voltages) under noise and harmonic distortion is substantial. There exists a need to acquire frequency estimates from all three phases simultaneously.

B.   Objective

Explore various frequency estimation algorithms and address the "trade-off"-s involved when proposing a viable solution that would meet basic requirements. Comprehend the computational difficulties in acquiring real-time estimates and simplify the estimation process for balanced three-phase systems

C.   My solution

Utilization of Clarke's Transformation to resolve three-phase signals to an equivalent complex exponential without any loss of information on the overall system frequency.

Implement a DFT-based iterative frequency estimation algorithm, and address all relevant design constraints.

Assess the estimator performance

D.   Contributions (at most one per line, most important first)

New estimation algorithm developed using the Clarke's Transformation and an iterative frequency estimator by interpolation of DFT coefficients

Demonstrated efficacy of solution

Addressed various "trade-off"-s and provided possible solutions

Lower complexity and Speedy Implementation

E.   Suggestions for future work

Cater to unbalanced conditions and harmonic distortion

Derive estimates of the phase at different locations on the loaded network

Smart Grid integration

While I may have benefited from discussion with other people, I certify that this thesis is entirely my own work, except where appropriately documented acknowledgements are included.

Signature: _Shafee_   Date: 30 / 10 / 2014

Thesis Pointers

List relevant page numbers in the column on the left. Be precise and selective: Don't list all pages of your thesis!

16	Problem Statement
16	Objective

Theory (up to 5 most relevant ideas)

15	Need for Three-Phase Power Frequency Estimation
21-23	Frequency Estimation of Sinusoids via Interpolation of DFT co-efficients
30-32	Clarke's Transformation

Method of solution (up to 5 most relevant points)

30-32	Utilization of Clarke's Transformation
33	Interpolation of DFT co-efficients to locate component frequency

Contributions (most important first)

34	New estimation scheme developed using the Clarke's Transformation and an iterative frequency estimator by interpolation of DFT coefficients
35-40	Demonstration and analysis of results
42-45	Development and Implementation of a novel test case

My work

30, 42-45	System block diagrams/algorithms/equations solved
35-40	Description of assessment criteria used
34	Description of procedure (e.g. for experiments)

Results

35-40	Succinct presentation of results
35-40	Analysis
41	Significance of results

Conclusion

46	Statement of whether the outcomes met the objectives
45	Suggestions for future research

Literature: (up to 5 most important references)

19-21	[3] E. Aboutanios, 2011
30	[22] E. Clarke, 1943
19	[12] D. Rife & R. Boorstyn

Acknowledgements

Abstract

The frequency of a three-phase power system serves as a fundamental parameter used to assess power quality and system health, and must be closely monitored and controlled to be within its specified operating limits. Power system protection and control applications, such as frequency relays for load shedding, load-frequency controllers, require accurate and fast estimation of the frequency, and hence has become a major field of research in recent years. Most digital algorithms developed thus far, have acceptable accuracy. However, the complexities involved in acquiring direct estimates from the phase voltages are significant, as none of the single phases can necessarily characterize the entire system and its properties.

This paper proposes a novel technique, that utilizes the powerful Clarke's (or $\alpha\beta$-) transformation to encompass the three-phase information within a single complex exponential. A frequency-domain estimator, that takes advantage of the highly efficient fast Fourier transform (FFT) algorithm, is then used to obtain estimates of the true system frequency at a high degree of precision.

List of Abbreviations

AC Alternating Current

AWGN Additive White Gaussia Noise

ZC Zero-Crossing

MLE Maximum Likelihood Estimate

CRLB Cramer Rao Lower Bound

DFT Discrete Fourier Transform

MBS Maximum Bin Search

RMSE Root Mean Square Error

SNR Signal-to-Noise Ratio

WLS Weighted Least Square

Contents

List of Figures

List of Tables

Chapter 1

Introduction

The power frequency is a measure of the number of oscillations of AC power in an electrical power grid, transmitted from the generation plant to the end user. In most parts of the world, it is rated at 50Hz, while 60Hz is also a typical value for regions such as the Americas, and parts of Asia.

1.1 Standardization of Power Frequency

The standardization of frequency in geographic areas has facilitated the interconnections of generators in a grid.
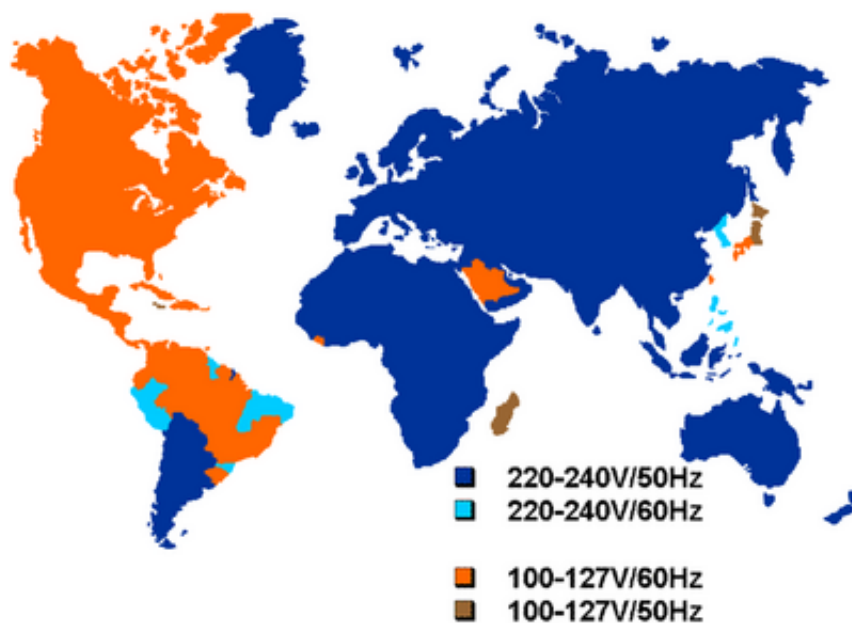
Figure 1.1: AC Frequency and Voltage by region [1]

Standard Power Frequency in Australia

The nominal AC frequency used in Australia is rated at 50Hz.

The frequency operating standards for both the mainland regions and the Tasmania region require that, during periods when there are no contingency events and no load events, the frequency be maintained within the range 49.85 to 50.15 Hz for 99% of the time, with larger deviations permitted within the range 49.75 to 50.25 Hz for no more than 1% of the time[5].

For an island within the mainland regions or an island within the Tasmania power system, the frequency operating standards require that, during periods when there are no contingency events and no load events, the frequencies be maintained within the ranges 49.5 to 50.5 Hz and 49.0 and 51.0 Hz respectively[5].

1.2   Power Quality and Frequency

Synchronization of AC voltage frequency and phase ensures reliable functioning of electrical power systems and the mitigation of performance losses and reduced system lifespan.

The term *power quality* is used to objectify the electric power that drives a load and the load's ability to function properly. Without proper monitoring and subsequent conditioning(if required) of power, an electrical device(or load) is bound for malfunctioning, premature failure or even start-up.

While tracking power quality, the measurement of the variation of frequency is a major area of concern.

1.3   Causes and Effects of Power Frequency Fluctuation

There are several distinguished events that may lead to a fluctuation in system frequency, some of which has been listed below:

- Generation and load imbalance: Most common in smart grids, due to the system's recurring switching between the main grid and microgrids, during which parts of the system completely switches the main grid off (islanding).

- Single- and dual-phase faults: The occurrence of faults in one or two phases and sudden drops in voltage for a short period of time (also known as voltage sags)[6] will result in incorrect frequency estimates and henceforth, cause an alarm to spread throughout the system. In the subsequent sections of this report, we will learn how the frequency of a three-phase power system is derived from the relationship between each of the phase voltages.

- Duality of load-supply: Again, most common in smart grids where dynamic loads and dual load-generator devices, such as plug-in electric vehicles(PEVs), which can give back energy to the grid in case of an emergency, are deployed. Drifting of reactive power

which results from frequent switching, causes oscillations of power levels and harmonics in frequency.

- Introduction of harmonics: This problem mainly arises due to the non-linear V-I characteristics of certain loads (power supplies, semiconductor rectifiers, motors, electric arc furnaces)which give rise to harmonics, which may be non-integer multiples of system frequency. This leads to resonance in the system leading to significant rise in currents and overheating of transformers [7]. The operation of shunt capacitors for reactive power compensation also propagates strong transients and harmonics that eventually leads to equipment damage.

- Stability issues: In the event of faults or short circuits, power system instability becomes an issue and in order to solve the consequent problems, accurate frequency estimation is required to facilitate actions such as load(or generator) shedding.
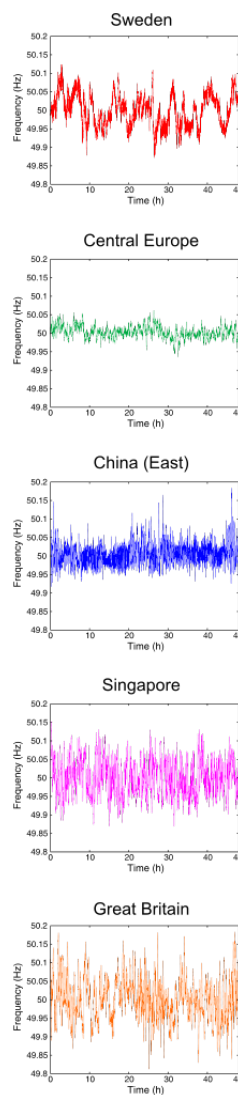
Figure 1.2: Power Frequency Fluctuation in some of the world's largest power grids [2]

14

1.4 Frequency Estimation for Power Systems

The estimation of a power system's operating frequency is one of the most important areas of research, as it provides a reflection on the dynamic energy balance between generation and consumption. Frequency deviation must, therefore, be carefully monitored and controlled in order to kept within certain operating bounds.

In power systems, the core purpose of frequency estimation is for designing schemes and/or further equipment to provide protection against loss of synchronism, under-frequency relaying, and facilitate power system stabilization following transient events [8]. In order to enhance fault identification and subsequent troubleshooting in a power system, there is a demand for a unified frequency estimation platform in three-phase power systems, exhibiting the following characteristics [9]:

- demonstrate resilience towards noise and harmonics in the system, including the ones that are not integer multiples of the system frequency;

- real-time adaptive, fast converging and asymptotically unbiased;

- real-time performance must be as close to theoretical limits as possible with minimum variance;

- capable of catering towards both balanced and unbalanced conditions.
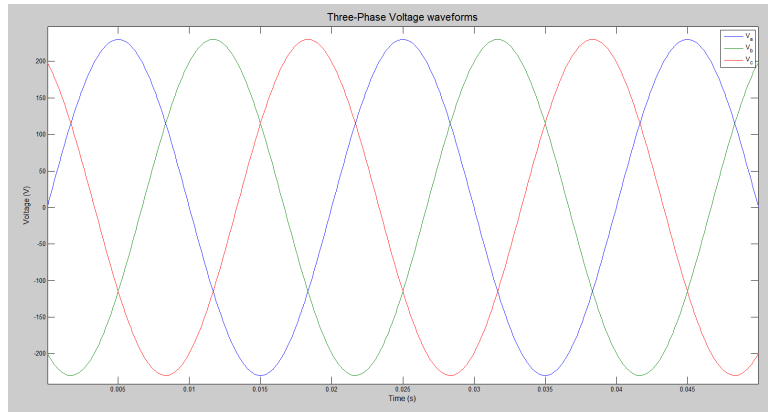
Figure 1.3: Three-phase waveforms

1.5 Generic Signal Model in a Three Phase System

For the purpose of this thesis, it is safe to assume that the three-phase power system operates under *balanced* conditions. The three-phase voltage signals can then be modelled in discrete time form as:

$$v_a(k) = V_a(k)\cos(\omega k\Delta T + \phi) + \epsilon_a(k)$$

$$v_b(k) = V_b(k)\cos(\omega k\Delta T + \phi - \frac{2\pi}{3}) + \epsilon_b(k) \qquad (1.1)$$

$$v_c(k) = V_c(k)\cos(\omega k\Delta T + \phi + \frac{2\pi}{3}) + \epsilon_c(k)$$

where $V_a(k)$, $V_b(k)$, $V_c(k)$ are the maximum values for the voltages in each phase at time instant k, ΔT is the sampling interval, ϕ is the phase of the fundamental component, $\omega=2\pi f$ is the angular frequency of the voltage signal, f is the system frequency, and $\epsilon_a(k)$, $\epsilon_b(k)$, $\epsilon_c(k)$ make up the noise components in each phase at the same time instant k. These latter terms are generally taken as Additive White Gaussian Noise (AWGN), having a variance of $\sigma^2/2$ [3].

Research on frequency estimation of power systems has been conducted for a long period of time, and as indicated before, is a key area of interest. Several different methods have been proposed thus far, along with in-depth coverage of their modelling techniques, results and performance attributes.

1.6   Problem Definition

Estimation of a three-phase AC power system's operating frequency provides a reflection on power quality and system health. The difficulty in acquiring such an estimate from each individual phase voltages(as well as line-to-line voltages) under noise, and harmonic distortion is substantial. There exists a need to acquire frequency estimates from all three phases simultaneously.

1.7   Thesis Objectives

- Understand the importance of power system frequency and its effects on system health and operation;

- Conduct an extensive background research on frequency estimation techniques designed specifically for implementation in three-phase power systems;

- Explore various frequency estimation algorithms and address the "trade-off"-s involved when proposing a viable solution that would meet basic requirements;

- Comprehend the computational difficulties in acquiring real-time estimates and simplify the estimation process for balanced three-phase systems;

- Acquire results from the proposed algorithm and forge methods for further refinement;

- Expose the proposed solution to a variety of contingency events and assess the subsequent performance; and,

- Lay the foundation for future work to be conducted in this particular field of research

1.8 Report Format

This paper, has been organized in the following manner:

- Chapter 2 (*Background*): is dedicated to provide analysis of existing frequency estimation algorithms

- Chapter 3 (*Methodology*): proposes a new technique in estimating the frequency of three-phase power systems and contains a step-by-step implementation plan of the design

- Chapter 4 (*Results*): contains results obtained from simulation, and addresses a few design constraints that must be catered to for optimized performance

- Chapter 5 (*Conclusion*): provides an overall review of this paper, in addition to stating the goals for future research and work.

Chapter 2

Background

2.1 Estimation Algorithms for Sinusoids

2.1.1 Method based on the Zero-crossing Technique

The zero-crossing (ZC) estimator operates by detecting zero crossings in the real and imaginary components of a complex exponential and storing the estimated time and phase of these zero crossing points to a coordinate set S as,

$$S = \{(t_1, \phi_1) \dots (t_L, \phi_L)\} \tag{2.1}$$

where L is the number of detected zero crossings. The ZC estimate is the obtained by performing linear regression on the coordinate set S. In order to improve the accuracy of the detection of zero-crossings and reduce computational complexities, the use of a sequential implementation model on a sample-by-sample basis is more preferred [10].

This method employs the use of *tracking variables*, *A-E* which are initially set to 0, and based on the appearance of a zero-crossing coordinate, (t_i, ϕ_i) are updated as follows:

$$
\begin{aligned}
A &= A + t_i^2 \\
B &= B + 1 \\
C &= C + t_i \\
D &= D - t_i\phi_i \\
E &= E - \phi_i
\end{aligned}
\tag{2.2}
$$

At any time, the zero-crossing phase and frequency estimates, $\hat{\phi}_{ZC}$ and $\hat{\omega}_{ZC}$, can be obtained

directly from the tracking variables as,

$$\hat{\phi}_{ZC} = intercept = -\frac{EA - CD}{BA - C^2} \tag{2.3}$$

$$\hat{\omega}_{ZC} = slope = -\frac{C}{A}\hat{\phi}_{ZC} - \frac{D}{A} \tag{2.4}$$

As refinements to such a highly adaptive technique to be utilized for frequency estimation, the use of **local linear regression**, and **pre-filtered observations** have been suggested. The details of such methods are, however, deemed as rather less useful in order to estimate for three-phase power signals.

Other variations of the ZC estimator, such as the one described in literature [11] have been implemented to estimate the frequency of electrical grids by reducing factors such as noise and other impulsive disturbances via the design and use of an adaptive multi-stage digital filter.

2.1.2   Methods based on the Maximum Likelihood Estimate

The signal model for use in this technique is given by,

$$x[k] = s[k] + w[k] = Ae^{(-\eta + j2\pi f)k} + w[k], \text{ for } k = 0....N-1 \tag{2.5}$$

where A is the complex amplitude, f is the signal frequency and η is the decay factor. For the purpose of this estimator, f is normalized to the sampling rate such that $f \in [-0.5, 0.5]$ is ensured. The $w[k]$ terms represent AWGN with characteristics as stated previously in section 1.5.

As proven in [12], the MLE of the frequency is given by the maximiser of the periodogram,

$$\hat{f}_{ML} = \arg\max_{\lambda} I(\lambda) \tag{2.6}$$

where the periodogram is defined as $I(\lambda) = |X(\lambda)|^2$ for,

$$X(\lambda) = \sum_{k=0}^{N-1} x[k]e^{-j2\pi k\lambda} \tag{2.7}$$

where N is the number of observed samples.

Given a block of N samples, the MLE of the frequency is the value that maximises the probability of actually obtaining these N samples when the measurements are performed.

The MLE is consistent under Gaussian Noise conditions due to its unbiased nature and achieves the lowest variance than any possible estimator[3].

The Cramer Rao Lower Bound

The Cramer Rao Lower Bound (CRLB) provides a benchmark to assess the performance of an estimator, setting a lower bound on the estimation variance. For any frequency estimator, the estimation variance σ_f^2 must satisfy the inequality $\sigma_f^2 \geq \tilde{\sigma}_f^2$, [12] where,

$$\tilde{\sigma}_f^2 = \frac{6f_s^2}{(2\pi)^2 \rho N(N^2 - 1)}. \tag{2.8}$$

Optimal Estimation Variance

In the event when noise terms may happen to be greater than the signal component, an outlier emerges, with a probability of occurrence, q_n.

In the event of an outlier emergence, any of the bins corresponding to $f \in [-0.5, 0.5]$, are equally likely to be chosen, and the resulting variance is due to the uniform distribution along the estimation interval, giving it a value of $1/12$.

The optimal estimation variance is given by combining the CRLB and the probability of occurence of the outlier, q_N to denote the lower bound on the performance. If the *maximum bin* is correctly chosen, then the error of estimation is completely confined within the main lobe and the variance is lower bounded by the CLRB, with a probability of $1 - q_N$.

In the event of an outlier emergence, any of the bins corresponding to $f \in [-0.5, 0.5]$, are equally likely to be chosen, and the resulting variance is due to the uniform distribution along the estimation interval, giving it a value of $1/12$.

Combining the CRLB, q_N (as formulated in [12]) and the above stated conditions, the total mean squared error now becomes,

$$\sigma_{TOT}^2 = q_N \frac{1}{12} + (1 - q_N)\frac{6}{(2\pi)^2 \rho N(N^2 - 1)} \tag{2.9}$$

Note: *Any good estimator presumably needs to have a threshold as near as possible to that of the MLE and an estimation variance above it that is as close as possible to the CRLB.*

2.1.3　Zero-Padded DFT

A regularly sampled grid utilizing the DFT can be defined as,

$$X[n] = \sum_{k=0}^{N-1} x[k]e^{-j2\pi k\frac{n}{N}}, \text{ for } k = 0....N - 1 \tag{2.10}$$

With an aim to mitigate the resolution problems of the MBS(resolution limited to $1/N$), the density of samples on the frequency axis is increased by padding the data with zeroes to some length $L \geq N$. This procedure leads to a more accurate location of the frequency much closer to the true maximum.

This is known as the zero-padded or ZP(L) estimator with an improved resolution of $1/L$. The signal frequency can then be measured as,

$$f = \frac{m + \delta}{L} \tag{2.11}$$

where $m = [Lf]$ is rounded to the nearest integer,and $-0.5 \leq \delta \geq 0.5$ is the frequency residual. Here, m serves the purpose of the bin index and δ represents the estimation error, uniformly distributed over $[-0.5, 0.5]$. The estimation variance is then,

$$\hat{\sigma}_f^2 = \frac{1}{12L^2} \tag{2.12}$$
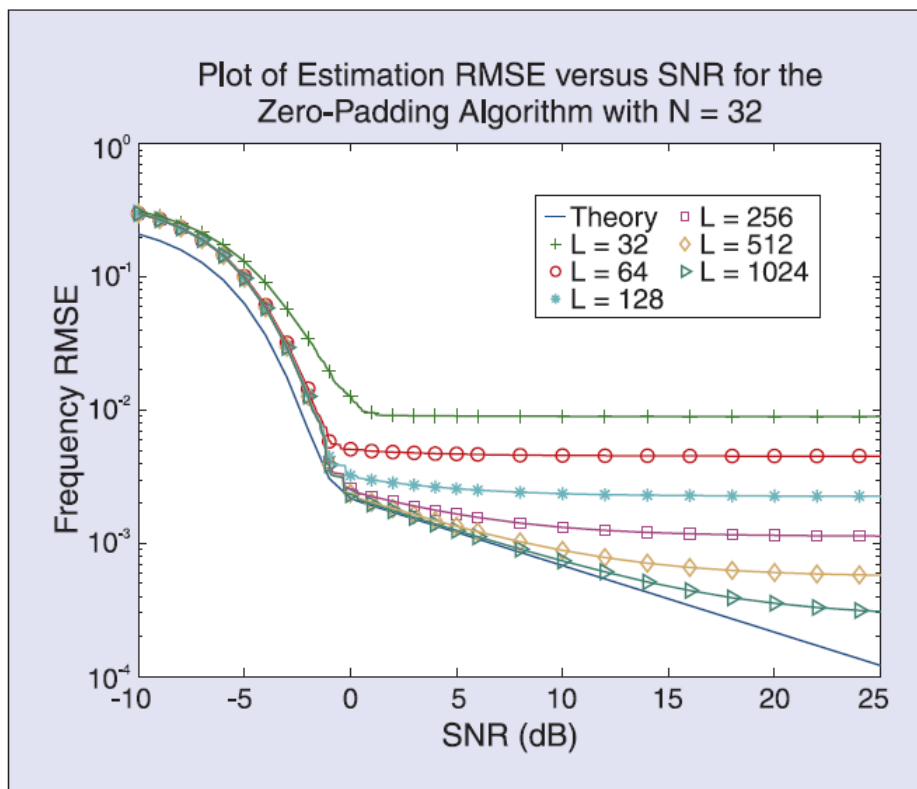
Figure 2.1: Plot of the performance of the zero-padding estimator as a function of signal to noise ratio [3]

As seen in Fig. 2.1, the ZP(L) algorithm has the worst threshold and the estimates have a much poorer CRLB for any viable SNR above the threshold even for $L = 1024$.

The performance can be improved with increasing L but has the downside of adding to computational cost, especially in real-time scenarios.

2.1.4   Interpolation of DFT coefficients

The previously highlighted problem with using the ZP(L) algorithm can be overcome by using interpolation to locate the the true maximum of $I(\lambda)$ and produce a *finer* estimate. Such a method has been extensively investigated in [12], [13], [14] and [15].

Two new coefficients, $X_p \equiv X[m + p]$, on the edges of the maximum bin, for $p = \pm 0.5$ and $m \equiv$ the index of the coarse estimate, evolve to interpolate the location of the maximum. For $|\delta| \leq 0.5$, the use of the approximation, $e^{j2\pi \frac{\delta}{N}} \approx 1 + j2\pi \frac{\delta}{N}$, results in a fine estimate of the residual frequency, $\hat{\delta}$ given as,

$$\hat{\delta} \approx h(\delta) = \frac{1}{2} \frac{X_{0.5} + X_{-0.5}}{X_{0.5} - X_{-0.5}} \tag{2.13}$$

It is worth noting that the above approximate relationship is permitted by the fact that $\frac{2\pi\delta}{N} \ll 1$, and since δ is real valued, on the real part of the interpolation function $h(\delta)$ is taken into consideration. The mentioned approximations required to formulate equation 2.13 produce a negligible bias as it is lower than the CRLB except in very large SNRs.

At very large SNRs, the finer estimate can be given as,

$$\hat{\delta} = \frac{N}{2\pi} \angle \hat{z} \tag{2.14}$$

where,

$$\hat{z} = \frac{1}{\cos(\frac{\pi}{N}) - 2jh(\delta)\sin(\frac{\pi}{N})} \tag{2.15}$$

It is worth understanding that, in the last iteration of this two-step strategy, the estimation variance converges to its minimum value as $\delta = 0$.
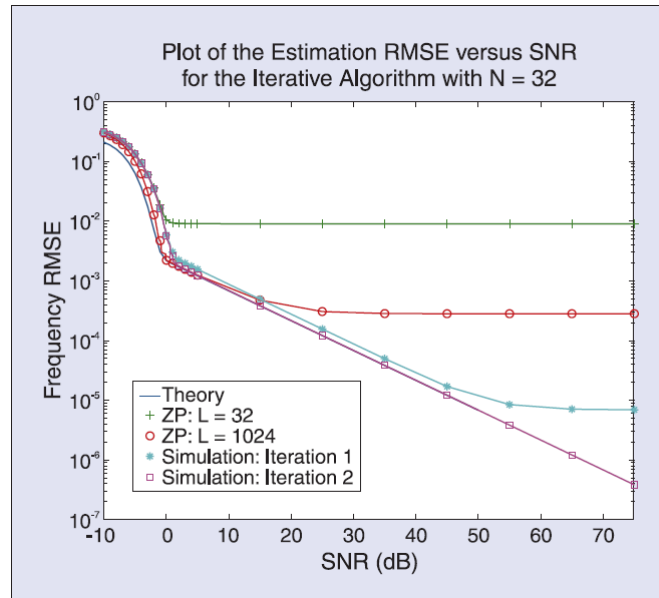
Figure 2.2: Performance of the iterative algorithm as a function of signal-to-noise ratio [3]

From Fig. 2.2 the elimination of the estimation floor (due to the estimation bias) between the first and second iterations is observed.

2.2 Conventional Three-Phase Frequency Estimation Techniques

2.2.1 Frequency Estimation of Three-Phase Power Systems based on the Weighted-Least-Square Algorithm and Adaptive FIR Filtering

The weighted-least-square(WLS) algorithm for frequency estimation has been effortlessly extended for use in three-phase power systems [16]. The following technique is considered to be robust as the estimated frequency is evaluated using the information contained within the three-phase voltage signals.

The measured three-phase signal model used here is as follows:

$$
\begin{aligned}
v_{a,i} &= V_a \cos(\omega_1 i \Delta t + \varphi_a) + \xi_{a,i} \\
v_{b,i} &= V_b \cos(\omega_1 i \Delta t + \varphi_b) + \xi_{b,i} \\
v_{c,i} &= V_c \cos(\omega_1 i \Delta t + \varphi_c) + \xi_{c,i}
\end{aligned}
\tag{2.16}
$$

where, $v_{a,i}$, $v_{b,i}$, $v_{c,i}$ are the sampled signal values in phases a, b and c;

V_a, V_b, V_c are the signal amplitudes in each phase;

φ_a, φ_b, φ_c are the phases of signals in each phase;

$\xi_{a,i}$, $\xi_{b,i}$, $\xi_{c,i}$ are the noise terms in each phase;

ω_1 is the system frequency;

$i \Delta t$ is the discrete time instant.

2.2.1.1 Prefiltering of signals

FIR digital filters are used to process the input phase voltage signals and eliminate and/or minimize the effects of noise whilst being unaffected by the presence of undesirable harmonics [4]. The most fundamental requirement to be met while designing such filters is that the filter must have nulls at the harmonic frequencies that are "expected" to be present in the signal. In iterative frequency estimation techniques such as the one to follow in the next subsection, the filters are required to adapt to each iteration as their gains are frequency-dependant.

As discussed in [17] and [18], the filter coefficients are calculated in closed forms, and a complete filter is realized as a cascade of the second-order sections, with each section eliminating one of the harmonics. The complete cascade eventually filters out the dc component and all the harmonic frequencies except for the fundamental one. The section that eliminates the dc component, has unity gain at the fundamental angular frequency, and has a Z-domain transfer function [17] as follows:

$$
H_{01}(z) = \frac{1 - z^{-2}}{|1 - z_1^{-2}|}
\tag{2.17}
$$
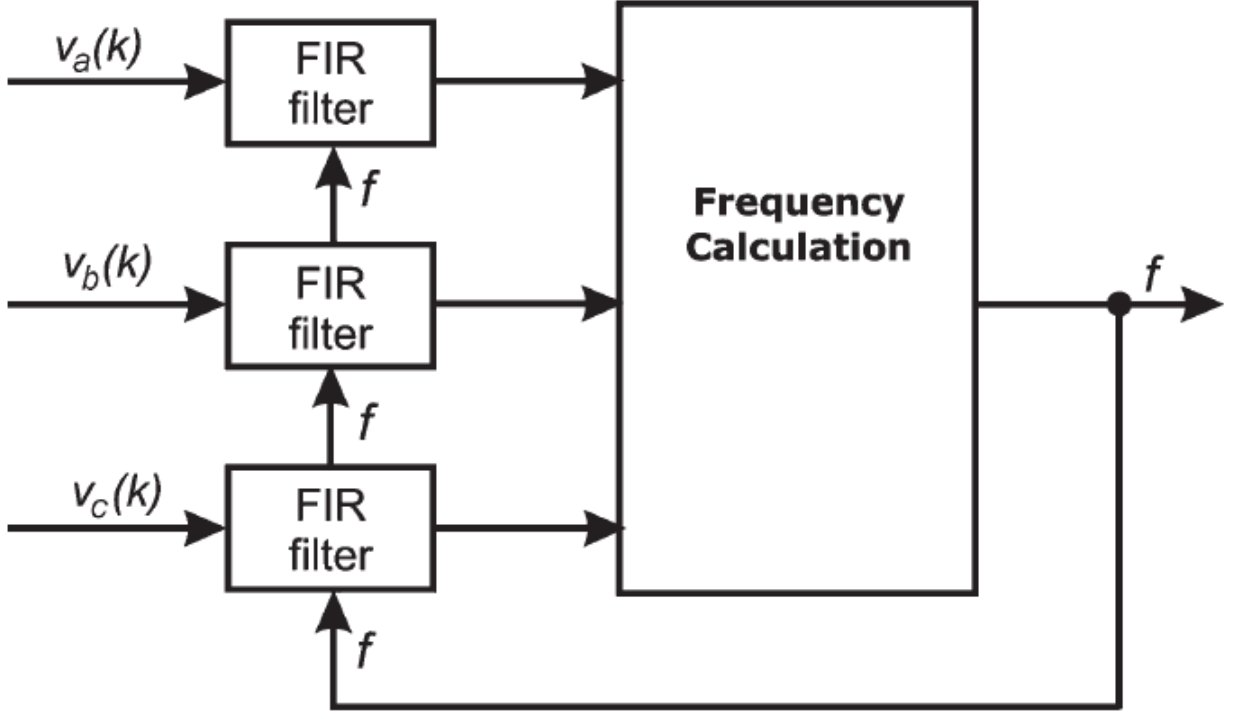
Figure 2.3: Block Diagram of the estimation scheme

where $z = exp(j\omega\Delta t)$, $z_1 = exp(j\omega_1\Delta t)$, and $|1 - z_1^{-2}| = 2\sin(\omega_1\Delta t)$.

The section that rejects the harmonic ω_i, also has a unity gain at the fundamental angular frequency, and its transfer function is given by [19]:

$$H_{1i}(z) = \frac{1 - 2\cos(\omega_i\Delta t)z^{-1} + z^{-2}}{|1 - 2\cos(\omega_i\Delta t)z^{-1} + z^{-2}|} \tag{2.18}$$

The complete filter's transfer function can now be given by[4]:

$$H_1(z) = H_{01}(z)\prod_{i=2}^{M} H_{1i}(z) \tag{2.19}$$

where, M denotes the maximum integer part of $f_s/(2f_1)$.

2.2.1.2 Estimation of Frequency

Three consecutive samples of the *prefiltered* signal in phase a are connected by the equation [16]:

$$\frac{v_{a,i} + v_{a,i-2}}{2} = v_{a,i-1}\cos(\omega_1 i\Delta t) \tag{2.20}$$

or

$$y_{a,i} = z_{a,i}x \tag{2.21}$$
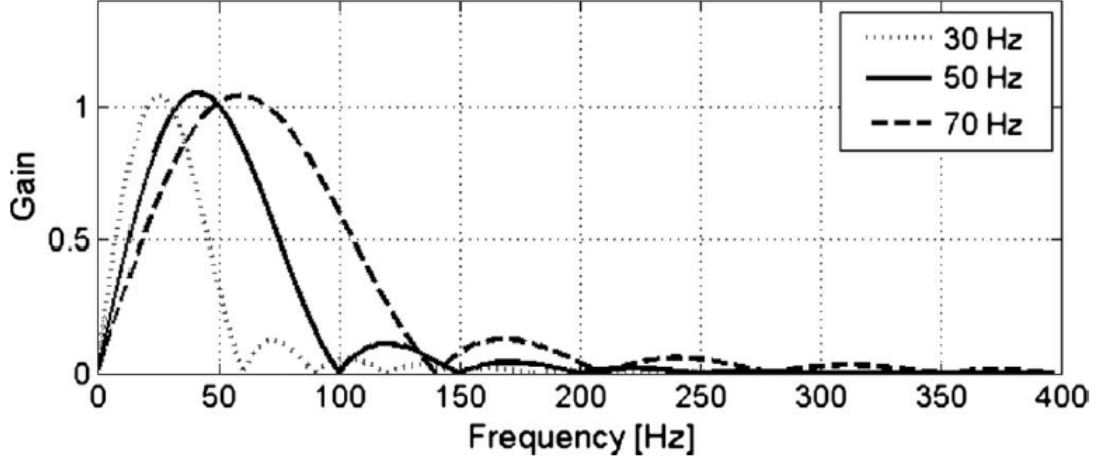
Figure 2.4: Frequency responses of the first harmonic filter for different fundamental frequencies and a sampling frequency of $f_s = 800$ Sa/s (used for picture clarity) [4].

where,

$$y_{a,i} = \frac{v_{a,i} + v_{a,i-2}}{2},$$

$$z_{a,i} = v_{a,i-1} \tag{2.22}$$

$$x = \cos(\omega_1 i \Delta t)$$

The above equations, similarly also hold true for phases b and c. A system of linear equations is then formed, by substituting $i = 1,2,...,k$ $(k > 2)$:

$$\mathbf{y_k} = \mathbf{z_k} x_k \tag{2.23}$$

A "forgetting factor", $0 < W < 1$, is introduced in the the $\mathbf{y_k}$ matrix in order to reduce the significance of *older* data and enhance that of *newer* samples. The value of W plays a rather prominent role in the estimator performance, as the closer it is to 1, the more accurate the estimator would become, however with a lower convergence rate, and vice versa.

The solution to 2.23 at any instant k, as per the least-error-square method is given by,

$$x_k = (\mathbf{z_k^T z_k})^{-1} \mathbf{z_k^T y_k} \tag{2.24}$$

As shown in literature [4], the solution x_k can be calculated using the following formula:

$$x_k = \frac{\sum_{i=0}^{k} \{W^{2(k-i)}[z_{a,i} y_{a,i} + z_{b,i} y_{b,i} + z_{c,i} y_{c,i}]\}}{\sum_{i=0}^{k} \{W^{2(k-i)}[z_{a,i}^2 + z_{b,i}^2 + z_{c,i}^2]} \tag{2.25}$$

Evaluation of x_k from equation 2.25 can now lead to the calculation of system frequency,

25

which is given by:

$$f_k = \arccos(x_k)/(2\pi\Delta t) \tag{2.26}$$

As highlighted before, there must be a compromise between accuracy and convergence in order to assign a value to W^2 during this estimation procedure.

(a)

(b)
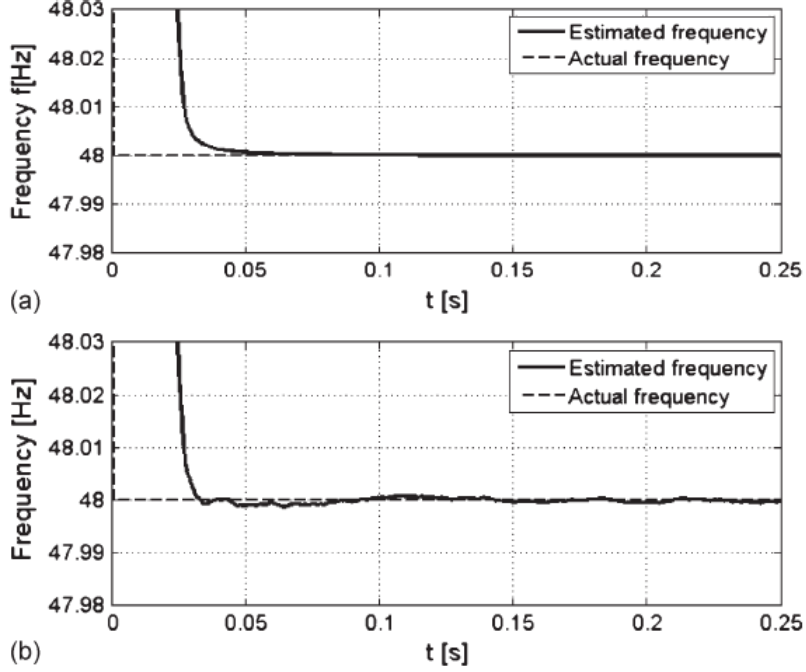
Figure 2.5: Estimations for $f = 50$ Hz for $t < 0$ s and $f = 48$ Hz for $t > 0$ s, with the presence of harmonics and (a) without noise and (b) with SNR $= 60$ dB. [4]

2.2.2   Method Based on the Discrete Fourier Transform

The definition of frequency, as the angular velocity of the rotating voltage phasor [20], acts as the base for such a technique which involves the calculation of the phasor of the fundamental voltage waveform from N samples and using the DFT.

If the sampling interval equals one cycle of the basic waveform, the phasor at the time $t_k = kT$ is given in [21] as,

$$\mathbf{G}_k = \frac{2}{N} \sum_{n=0}^{N-1} v_{k+n-N+1} e^{-j\omega Tn} \tag{2.27}$$

where, T is the sampling interval, ω is the fundamental frequency and $v_{k+n-N+1}$ represents the sampled values of a voltage.

Upon execution, $\mathbf{G}_k$ is updated at every sampled value, with each new value obtained after the sampling interval taken into calculation while the oldest one is neglected. The instantaneous frequency can be calculated from two consecutive phasors

$$\omega = \frac{\arg[G_{k+1}] - \arg[G_k]}{T} \tag{2.28}$$

where,

$$\arg[G_k] = \tan^{-1} \frac{\text{Im}[G_k]}{\text{Re}[G_k]} \tag{2.29}$$

2.2.2.1 Filtering

A voltage waveform, taken from a voltage transformer, is required to be filtered using algorithms based on the DFT. The filter algorithm is given as,

$$g_k = \frac{2}{N} \sum_{n=0}^{N-1} v_{k+n-N+1} \cos(n\omega T) \tag{2.30}$$

It is worth noting that this only requires the time function of the fundamental component of the voltage to be equal to the real part of the phasor [20].

In order to improve the filter properties, especially addressing frequency changes, the application of a smoothing window is proposed, and as such, investigations were conducted on two very common window functions:

- Hamming Window, which is given by:

$$w_H = 0.54 - 0.46 \cos \frac{2\pi n}{N-1} \tag{2.31}$$

- Blackman Window given as:

$$w_B = 0.42 - 0.5 \cos \frac{2\pi n}{N-1} + 0.08 \cos \frac{4\pi n}{N-1} \tag{2.32}$$
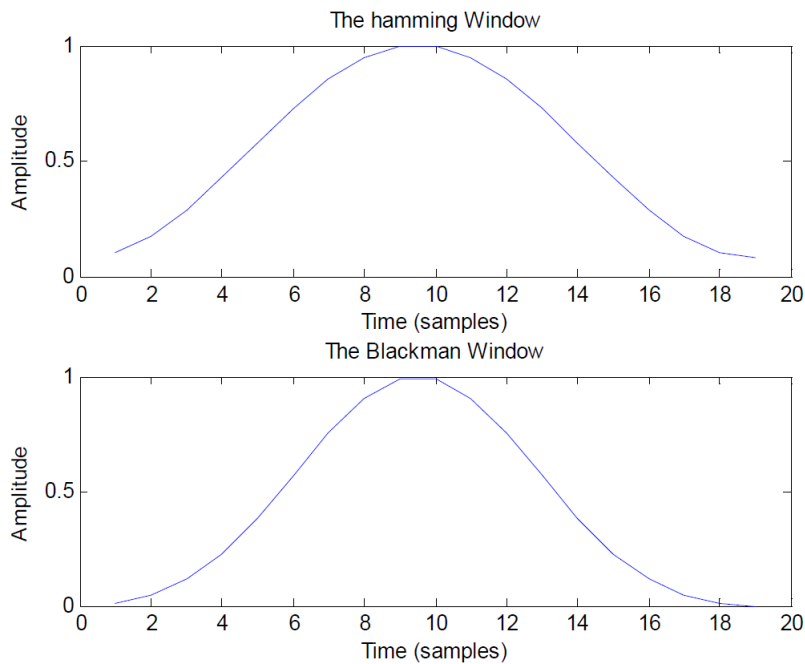
Figure 2.6: Amplitude Response of the Hamming and Blackman windows with N = 20

The core aim of the pre-filtering is to improve the accuracy of the frequency determination.

2.2.2.2 Algorithm Based on Prony's Estimation Method

Samples of the fundamental component of a voltage waveform are extracted at the output of the filter, and an algorithm based on Prony's estimation method is proposed for the evaluation of the system frequency. Prony's estimation method, works under the assumption that given a series of samples, g_1, g_2,......,g_M, a single sinusoid can be used to approximate a filtered voltage waveform,

$$y_m = A\cos(m\omega T + \psi) \tag{2.33}$$

for $m = 1, 2, \ldots M$, where M is the total number of samples taken into the approximation. Equation 2.33 can be rewritten in complex exponential form as,

$$y_m = bz_1^m + b^* z_1^{*m} \tag{2.34}$$

where,

$$z_1 = e^{j\omega T} \tag{2.35}$$

$$b = \frac{A}{2}e^{j\psi} \tag{2.36}$$

The objective here is to find the values of b and z_1 so that the error,

$$\delta_m = g_m - y_m \tag{2.37}$$

is minimized. The principal idea of the Prony's estimation method is to transform this non-linear problem into a linear fitting problem by minimizing the error E defined as,

$$E = \sum_{m=p}^{M-1} (\varepsilon_m)^2 \tag{2.38}$$

where p is the number of exponents and ε_m is given by,

$$\varepsilon_m = \sum_{k=0}^{p} a_k \delta_{k+m-1} \tag{2.39}$$

The parameters, a_k are initially unknown and are related to the frequency of the sinusoid. Equation 2.34 is the solution to some linear constant co-efficient difference equation and in order to find the form of the difference equation, the polynomial $F(z)$ is defined for $p = 2$,

$$F(z) = a_0(z - z_1)(z - z_1^*) = 0 \tag{2.40}$$

28

It is evident that z_1 and z_1^* are the roots of the polynomial. Using equation 2.34, we can derive,

$$\sum_{k=0}^{2} a_k y_{k+m-1} = a_0 y_{m-1} + a_1 y_m + a_2 y_{m+1} = 0. \tag{2.41}$$

From equations (2.37) and (2.39) it follows that,

$$\varepsilon_m = \sum_{k=0}^{2} a_k(g_{k+m-1} - y_{k+m-1}) = a_0 g_{m-1} + a_1 g_m + a_2 g_{m+1}. \tag{2.42}$$

If z_1 is a root of the polynomial $F(z)$ with unit modulus, then z_1^{-1} is also a root, and the coefficients a_k are symmetric about a_1, i.e., $a_0 = a_2$. For convenience, $a_1 = 1$ is chosen that for $a_0 = a_2$, resulting in,

$$\varepsilon_m = g_m + a_0(g_{m-1} + g_{m+1}). \tag{2.43}$$

The minimization of E with respect to the unknown a_0 is achieved if,

$$\frac{\partial E}{\partial a_0} = \sum_{m=2}^{M-1} 2[g_m + a_0(g_{m-1} + g_{m+1})](g_{m-1} + g_{m+1}) = 0. \tag{2.44}$$

Solving this for a_0, polynomial $F(z)$ can be expressed as,

$$z^2 + \frac{1}{a_0}z + 1 = 0. \tag{2.45}$$

whereby, the roots are,

$$z_{1,2} = -\frac{1}{2a_0} \pm j\sqrt{1 - \frac{1}{4a_0^2}}. \tag{2.46}$$

From the definition of the roots, being,

$$z_{1,2} = e^{\pm j\omega T} = \cos(\omega T) \pm j\sin(\omega T) \tag{2.47}$$

the angular frequency can then be given by,

$$\omega = \frac{1}{T}\cos^{-1}\left\{ \frac{\displaystyle\sum_{m=2}^{M-1} (g_{m-1} + g_{m+1})^2}{2\displaystyle\sum_{m=2}^{M-1} g_m(g_{m-1} + g_{m+1})} \right\} \tag{2.48}$$

This algorithm was vigorously put under test on a computer by Lobos and Rezmer and according to literature [21], a very high level of accuracy was achieved utilizing the Blackman window as the pre-filter for heavily distorted voltage waveforms.

Chapter 3

Methodology

The methods covered in the preceding sections have all been verified to provide accurate estimates of the frequency of the sinusoid(s), and the methods incorporated in their respective algorithms have been analysed to help better understand their behaviour.

In order to acquire frequency estimates for three-phase power systems that issues results with pin-point accuracy at a commendable processing speed, a new and innovative technique is now presented, whose design can be represented in the follwoing block diagram.
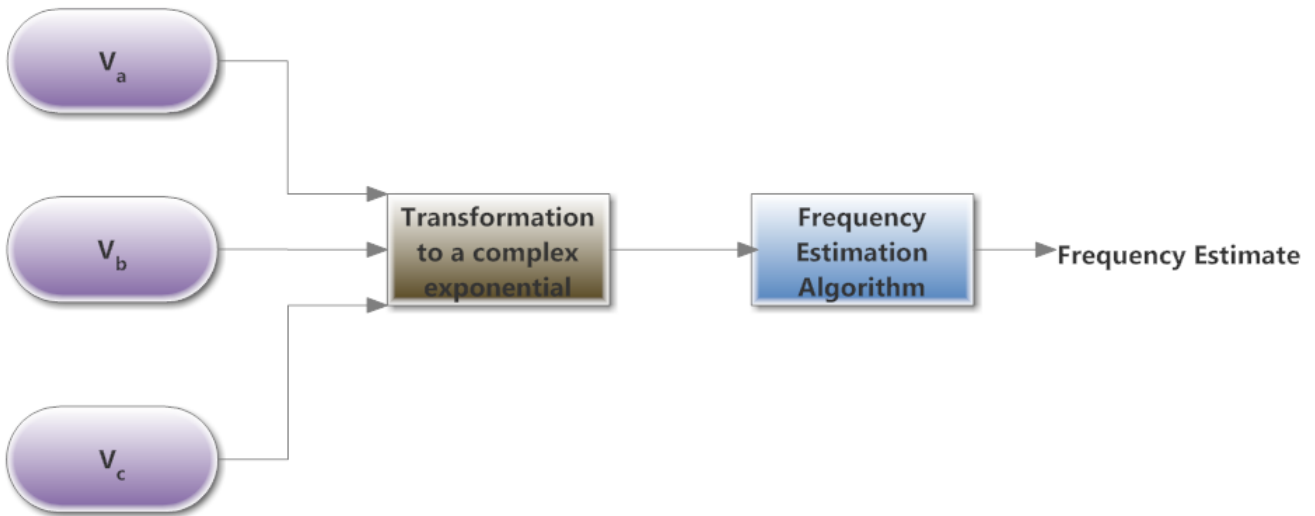
Figure 3.1: Block Diagram of the proposed solution

3.1 Transformation of a Three-Phase Signal

The three-phase signals are required to be transformed in order to facilitate the operation of frequency estimators on all three phases simultaneously. This is achieved via the $\alpha\beta$ -transform or, the Clarke's Transformation, developed by Edith Clarke [22]- one of the most popular and effective transformation techniques used worldwide.

This method, when invoked, essentially transforms the three-phase voltage variables into the zero-sequence (or DC), direct(α) and quadrature(β)-axis components, whilst preserving their amplitudes and other relevant information required for further analysis. This transformation is mostly employed when applying linear predictive modelling of three-phase voltages.

Equation 1.1 can then be put in the following matrix form:

$$
\begin{pmatrix} v_0(k) \\ v_\alpha(k) \\ v_\beta(k) \end{pmatrix} = \frac{2}{3} \begin{pmatrix} \frac{1}{2} & \frac{1}{2} & \frac{1}{2} \\ 1 & \cos(\frac{2\pi}{3}) & \cos(-\frac{2\pi}{3}) \\ 0 & \sin(\frac{2\pi}{3}) & \sin(-\frac{2\pi}{3}) \end{pmatrix} \times \begin{pmatrix} v_a(k) \\ v_b(k) \\ v_c(k) \end{pmatrix}
\tag{3.1}
$$

$$
\mathbf{v}_{0\alpha\beta} = \begin{pmatrix} v_0(k) \\ v_\alpha(k) \\ v_\beta(k) \end{pmatrix} = \frac{2}{3} \begin{pmatrix} \frac{1}{2} & \frac{1}{2} & \frac{1}{2} \\ 1 & -\frac{1}{2} & -\frac{1}{2} \\ 0 & \frac{\sqrt{3}}{2} & -\frac{\sqrt{3}}{2} \end{pmatrix} \times \begin{pmatrix} v_a(k) \\ v_b(k) \\ v_c(k) \end{pmatrix} = \mathbf{C}\mathbf{v}_{abc}
\tag{3.2}
$$

where $\mathbf{C}$ is the Clarke's transformation matrix.

Under sinusoidal and balanced conditions, it is clear that all of the components in (1.1) have the same amplitude,

$$
V_a = V_b = V_c = V
\tag{3.3}
$$

Considering $\phi = 0$ and substituting (1.1) in (3.1), the following can be deduced,

$$
\begin{pmatrix} v_0(k) \\ v_\alpha(k) \\ v_\beta(k) \end{pmatrix} = \begin{pmatrix} 0 \\ V\cos(\omega k \Delta T) \\ V\cos(\omega k \Delta T + \frac{\pi}{2}) \end{pmatrix}
\tag{3.4}
$$

Proceeding further on from here, and under the conditions stated in (3.3) and (3.4), it is denounced that $v_\alpha(k)$ and $v_\beta(k)$ are the orthogonal coordinates of a point whose variation in position proportional to the system frequency(to be estimated) and is, thereby, represented by [23]

$$
v(k) = v_\alpha(k) + jv_\beta(k)
\tag{3.5}
$$

where $j = \sqrt{-1}$. This representation of a signal is preferred as there is limited loss in information and also acts as the preferred signal in *adaptive* frequency estimation techniques.

Note: Refer to Appendix A for unbalanced conditions

Simplified Transformation

Under balanced conditions, the dc-component, i.e., $v_0(k)$ will equal zero and hence can be overlooked while attempting to form the complex exponential.

$$\mathbf{v}_{\alpha\beta} = \mathbf{C}_{\alpha\beta} \times \mathbf{v}_{abc} \tag{3.6}$$

or,

$$\begin{pmatrix} v_\alpha(k) \\ v_\beta(k) \end{pmatrix} = \begin{pmatrix} \alpha_a & \alpha_b & \alpha_c \\ \beta_a & \beta_b & \beta_c \end{pmatrix} \times \begin{pmatrix} v_a(k) \\ v_b(k) \\ v_c(k) \end{pmatrix} = \frac{2}{3} \begin{pmatrix} 1 & -\dfrac{1}{2} & -\dfrac{1}{2} \\ 0 & \dfrac{\sqrt{3}}{2} & -\dfrac{\sqrt{3}}{2} \end{pmatrix} \times \begin{pmatrix} v_a(k) \\ v_b(k) \\ v_c(k) \end{pmatrix} \tag{3.7}$$

The resulting orthogonal components $v_\alpha(k)$ and $v_\beta(k)$ are defined in terms of the phase voltages as follows:

$$v_\alpha(k) = \frac{2}{3}\left(v_a(k) - \frac{v_b(k) + v_c(k)}{2}\right) \tag{3.8}$$

$$v_\beta(k) = \frac{1}{\sqrt{3}}\left(v_b(k) - v_c(k)\right) \tag{3.9}$$

3.2 Frequency Estimation Algorithm

Although a copious body of literature has been published in recent years on frequency estimators having exceptional performance, the method to be proposed for this particular thesis invokes the use of an iterative algorithm by interpolation on Fourier coefficients of a discrete time complex exponential as reviewed in section 2.1.4.

The estimator consists of a coarse search (using standard MBS), followed by a fine search algorithm for the component frequency of the exponential. It is meant to be implemented iteratively and, as proven in its supporting literatures-[3], [13]- converges to the true signal frequency of a complex sinusoid with a minimum estimation variance whilst satisfying the CRLB requirements.

3.3 Verification of the Estimation Algorithm on an Arbitrary Complex Signal

Firstly, in order to get an impression of the iterative estimation algorithm's core performance attributes, a simple complex sinusoid having the following form was put under test:

$$x[k] = s[k] + w[k] = Ae^{(j2\pi\frac{f}{f_s})k} + w[k] \tag{3.10}$$

where, without loss of generality, the signal amplitude, A was set to unity, and the true signal frequency, f is normalized to the sampling rate, $f_s = 1$, such that $f \in [-0.5, 0.5]$. As previously defined , $w[k]$ terms represent AWGN.
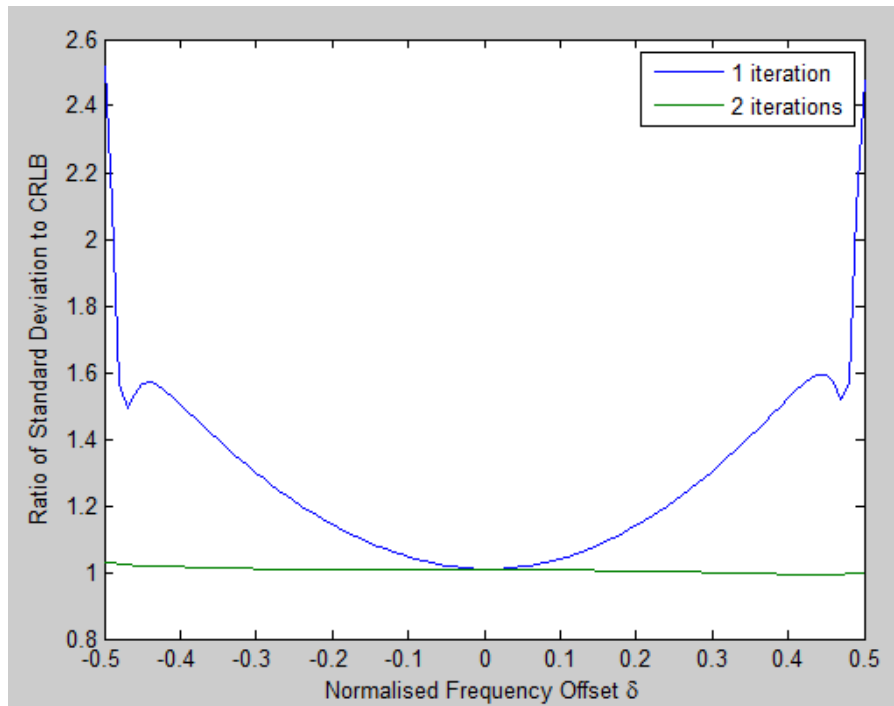
Figure 3.2: Plot of the ratio of the variance of the estimator to the asymptotic CRLB as a function of δ, which is the frequency offset from the bin center. Simulation curves for one and two iterations are shown.
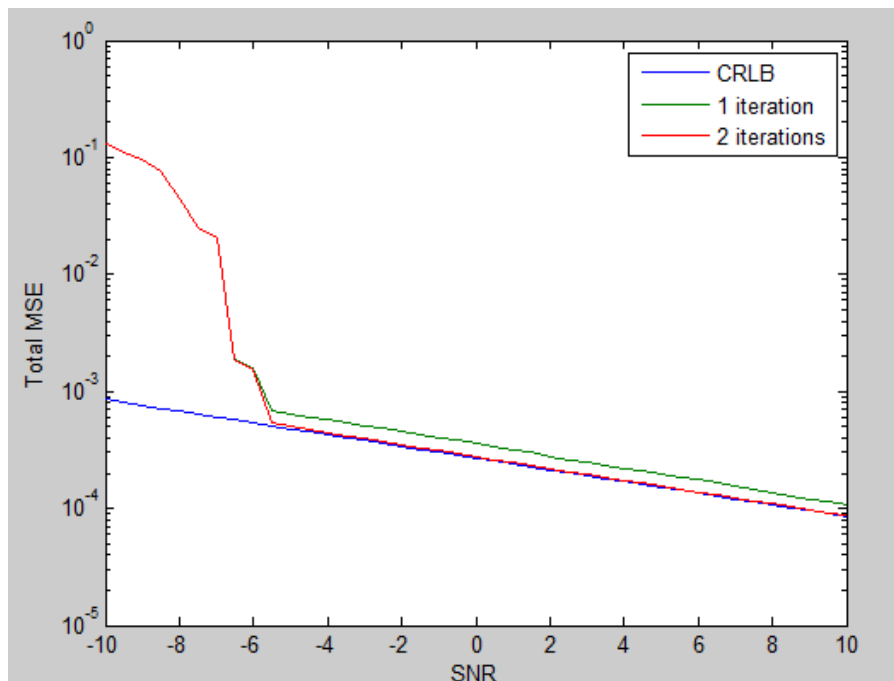
Figure 3.3: Plot of the standard deviation of the frequency estimation error as a function of the SNR. The CRB curve is also shown

The number of samples N used to test out the estimator was 128, although it remains to be seen how that would change in our overall method proposed in the previous chapter. Figure 3.2 shows the simulation results based on the ratio of the variance (of each iteration of the estimator) of the estimates to the CRLB. It does indicate that the true system frequency can

33

be reliably estimated from the centre of the maximum bin.

Figure 3.3 demonstrates the noise performance and unbiased nature of our chosen estimation algorithm as a function of the SNR, in that the two iterations converge to the theoretical CRLB curve, once the threshold effect (originating from the coarse estimation stage) subsides.

3.4   Implementation Plan

The following steps must be taken in order to realize the overall system design :

1. Construct sinusoidal waveforms corresponding to each phase of the three-phase voltage signals, adhering to the signal model as given by equation 1.1

2. Set sampling frequency, f_s

3. Obtain N samples of the three-phase voltages to visualize $\mathbf{v}_{abc}(k)$

4. Initialize the Clarke's transform matrix $\mathbf{C}$

5. Perform the transformation to yield $v_\alpha(k)$ and $v_\beta(k)$

6. Form the complex exponential, such that $v[k] = v_\alpha(k) + jv_\beta(k)$, for $k = 0...N-1$

7. Let $X = \text{FFT}(v)$,
   and $Y[n] = |X[n]|^2$, for $n = 0 \ldots N-1$

8. Locate the maximum bin:
   $m = \arg\max Y[n]$

9. Set $\hat{\delta} = 0$

10. Perform 1st iteration of Estimator Algorithm:
    $$X_p = \sum_{k=0}^{N-1} x[k]e^{-j2\pi k\frac{m+p}{N}} \text{, for } p = \pm 0.5$$
    $$\hat{\delta} = \frac{1}{2}\text{Re}\{\frac{X_{0.5} + X_{-0.5}}{X_{0.5} - X_{-0.5}}\}$$

11. Perform 2nd iteration of Estimator Algorithm:
    $$X_p = \sum_{k=0}^{N-1} x[k]e^{-j2\pi k\frac{m+p+\hat{\delta}}{N}} \text{, for } p = \pm 0.5$$
    $$\hat{\delta} = \hat{\delta} + \frac{1}{2}\text{Re}\{\frac{X_{0.5} + X_{-0.5}}{X_{0.5} - X_{-0.5}}\}$$

12. Acquire final frequency estimate:
    $$f = \frac{m + \hat{\delta}}{L}f_s.$$

Chapter 4

Simulation Results

This chapter investigates the project being put under test in the MATLAB environment, with each section also containing the assessment of the stated results.

4.1 Verification of Clarke's Transformation

The implementation of the Clarke's Transformation is quite straightforward in MATLAB to yield the complex exponential s.

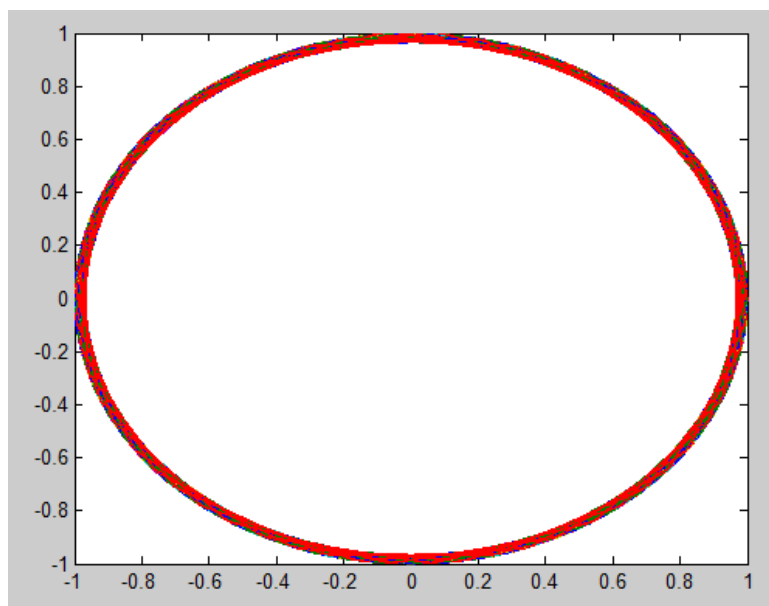Figure 4.1: Plot of the complex exponential s formed using the α and β components of output of the Clarke's Transformation

4.2 The Noiseless Case

In the case where we assume that no noise is present in the system, the implementation of our iterative estimator is deemed redundant as the system frequency will always converge to its true value at the center of the maximum bin in its frequency domain representation.

Figure 4.2: Plot of the ratio of the mean squared error of the estimator to the asymptotic CRLB as a function of δ, which is the frequency offset from the maximum bin center. Simulation curves for one and two iterations are shown.

The conclusion that can be drawn from the given plot is that, during the first iteration only, the mean squared error varies as we move away from the absolute center of the maximum bin in the frequency domain. The second iteration is shown to be redundant in this case, to further supplement our initial claim made at the start of this section.

4.3   Addition of Noise

Before revealing the performance of our estimation algorithm on the complex sinusoid(derived from the Clarke's Transformation output components), with added noise, it is only reasonable to revisit some basic principles to denote noise power.

The noise terms, $w[k]$ in our signal, $x[k]$ have zero mean and independent variance equivalent to $\sigma^2/2$ .Noise power, σ^2, is derived from the expression of the SNR, ρ, which is given by,

$$\rho = \frac{A^2}{\sigma^2} \tag{4.1}$$

where A represents the amplitude of our signal, $s[k]$ at any sampling instant, k. Rearranging the above equation yields,

$$\sigma^2 = \frac{A^2}{\rho} \tag{4.2}$$

For simulation purposes, the extent of noise is varied by altering the required SNR, ρ, while holding A to unity.

4.3.1 Performance of Estimator as a Function of δ

We now investigate and analyse the performance of our estimator under various noise conditions.

Sinusoid Under Heavy Noise

The number of samples taken is initially set to 128. We shall look at how the performance of the estimator implemented on a 'noisy' signal would vary with respect to the number of samples that are collected for analysis.
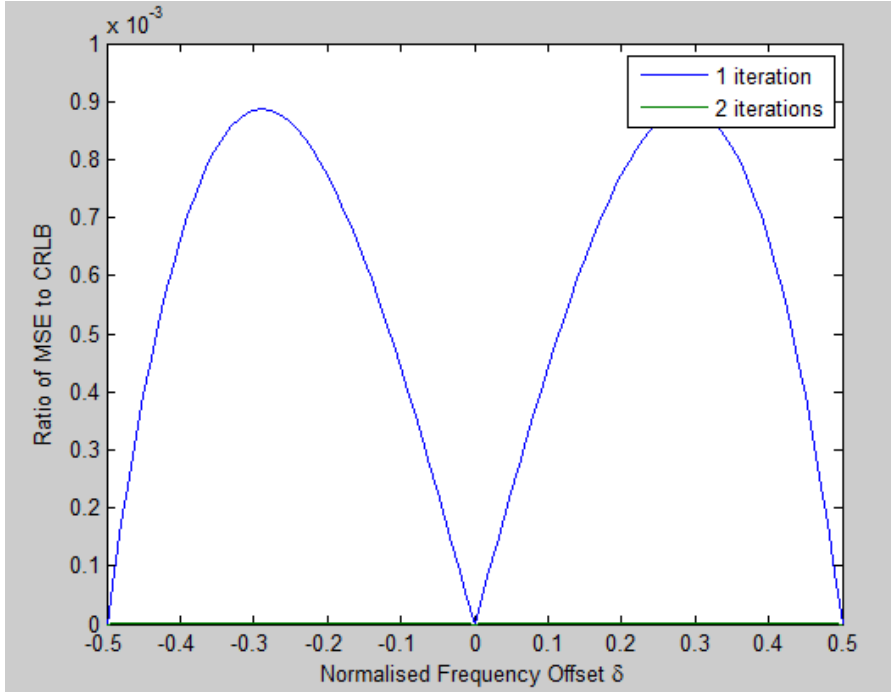

Figure 4.3: Plot of the ratio of the mean of acquired estimates to the asymptotic CRLB as a function of δ, which is the frequency offset from the maximum bin center. Simulation curves for one and two iterations are shown for $N = 128$

Figure 4.4: Plot of the ratio of the standard deviation of acquired estimates to the asymptotic CRLB as a function of δ, which is the frequency offset from the maximum bin center. Simulation curves for one and two iterations are shown for $N = 128$

The above plots demonstrate how the mean of the acquired frequency estimates approach the CRLB (meaning the ratio of the mean of estimates to the CRLB approaches zero) in addition to the standard deviation of the estimates converging to the asymptotic CRLB in the region closest to the peak of the maximum bin. It can be seen that the difference between the first iteration of the estimator and the CRLB 'floor' is eliminated once the second iteration is completed.

The number of samples is reduced then to 32 (a power of 2), hoping to increase the speed of convergence of the algorithm, and thereby reducing computational load.

Figure 4.5: Plot of the ratio of the mean of acquired estimates to the asymptotic CRLB as a function of δ, which is the frequency offset from the maximum bin center. Simulation curves for one and two iterations are shown for $N = 32$

Figure 4.6: Plot of the ratio of the standard deviation of acquired estimates to the asymptotic CRLB as a function of δ, which is the frequency offset from the maximum bin center. Simulation curves for one and two iterations are shown for $N = 32$

The difference in using two different values for the number of samples taken, is now clearly visible. Although the speed of evaluation has been enhanced, and hence, computational load has been decreased gravely, it is noticeable that reducing the number of samples, increases the adverse effects of the noise variance as we intend to move away from the center of the maximum bin that is most likely to entail the component frequency.

Now, let us increase N to 256 (another power of 2), at the expense of computational speed to further assess the accuracy of our estimates.
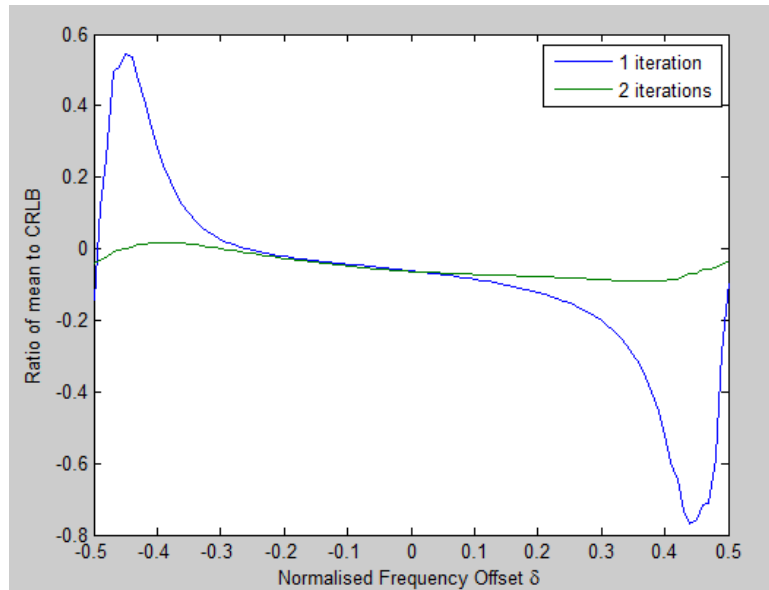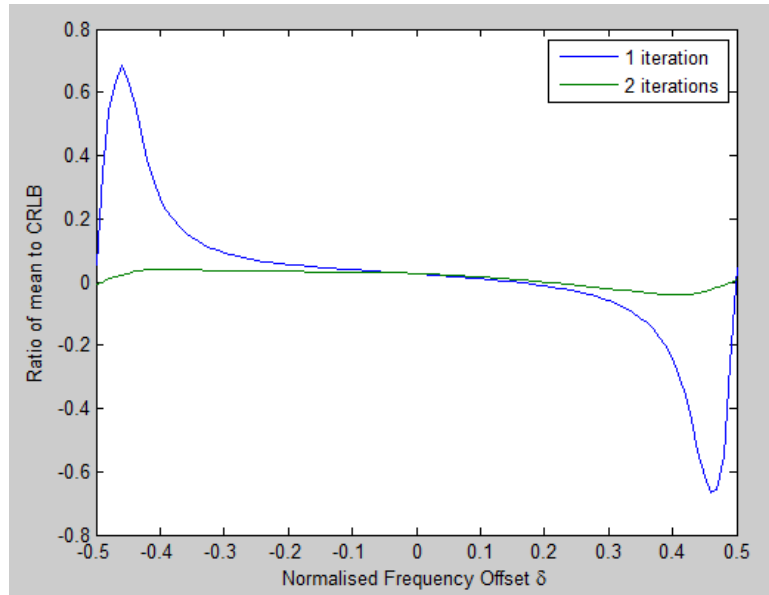

Figure 4.7: Plot of the ratio of the mean of acquired estimates to the asymptotic CRLB as a function of δ, which is the frequency offset from the maximum bin center. Simulation curves for one and two iterations are shown for $N = 256$
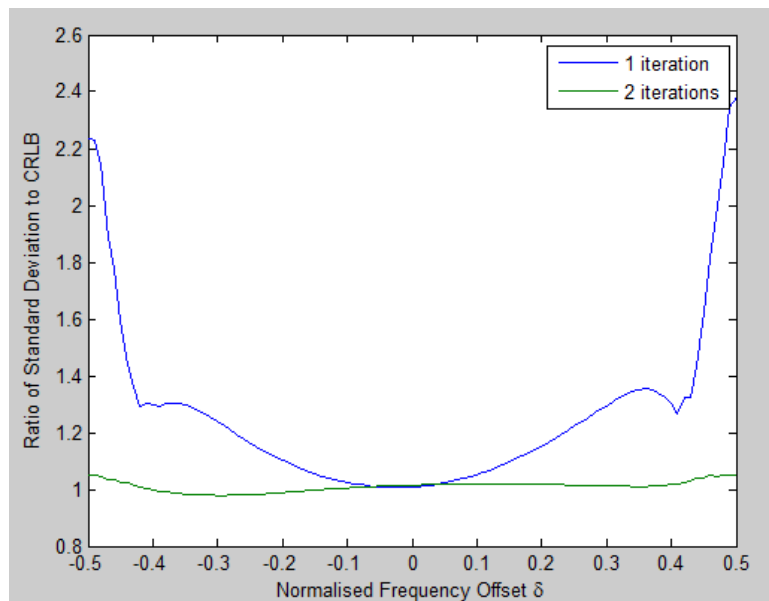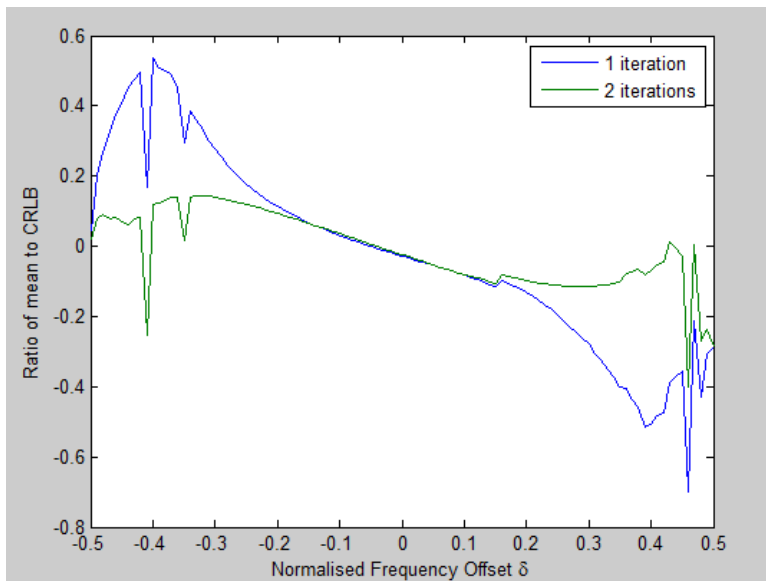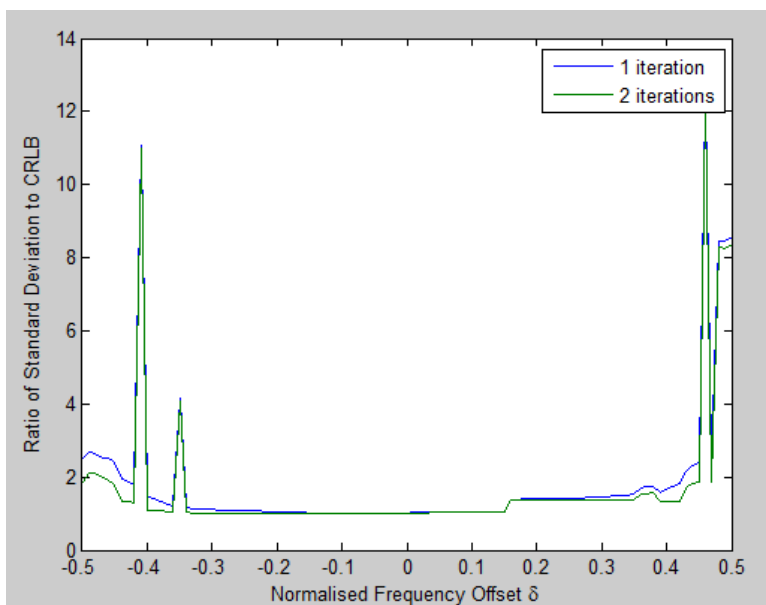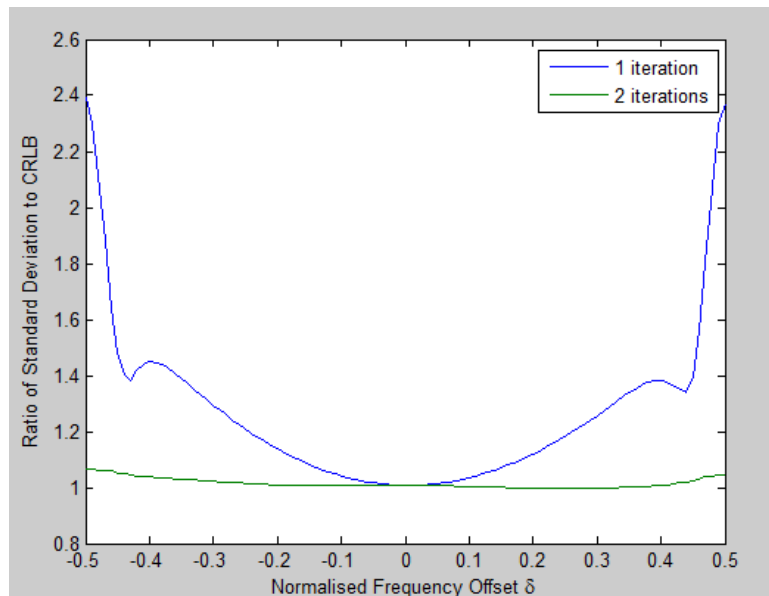

Figure 4.8: Plot of the ratio of the standard deviation of acquired estimates to the asymptotic CRLB as a function of δ, which is the frequency offset from the maximum bin center. Simulation curves for one and two iterations are shown for $N = 256$

The results, as seen now are much finer, with the second iteration of the estimator algorithm maintaining the CRLB requirement. One may assume that increasing N improves the accuracy of the estimation, at the expense of computational speed, but is not as desirable in real-time scenarios.

4.3.2 Performance of Estimator as a Function of SNR

We would now like to assess the quality of our frequency estimator based on its performances at varying SNRs and N.
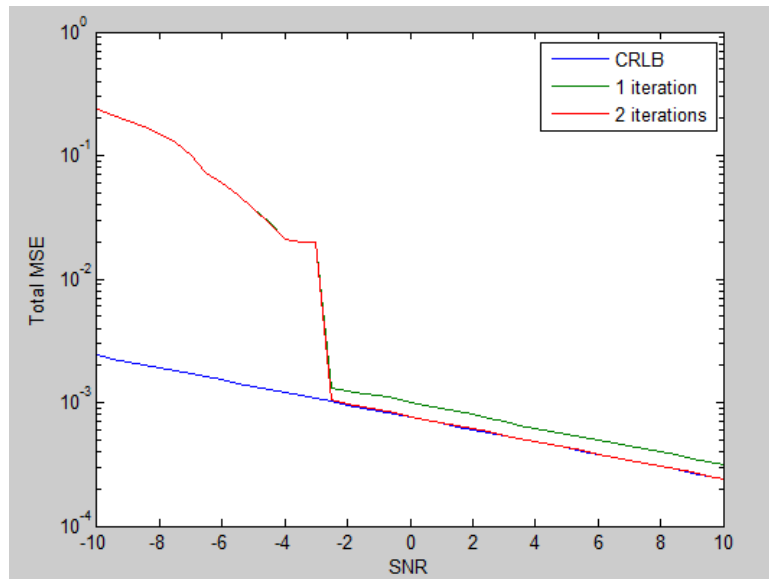
Figure 4.9: Performance of the estimator of the frequency as a function of the signal to noise ratio with N=64
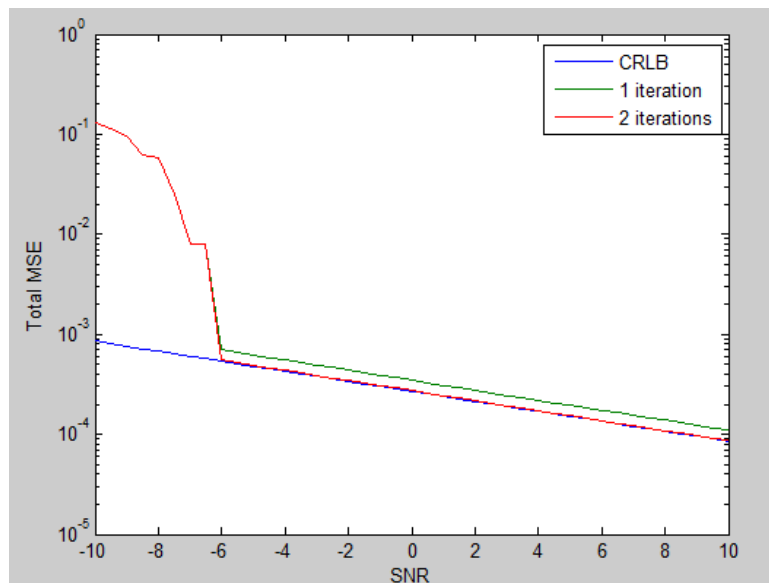
Figure 4.10: Performance of the estimator of the frequency as a function of the signal to noise ratio with N=128
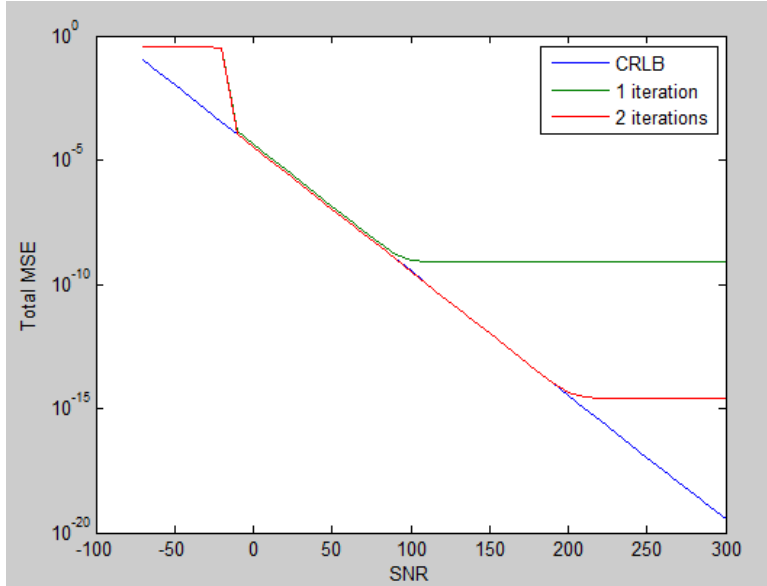
Figure 4.11: Performance of the estimator of the frequency as a function of the signal to noise ratio with N=512

To summarise the results, the performance floor between the first and the CRLB is eliminated by the second iteration at lower values for the SNR, with increasing N.

Although there is less variance in using larger number of samples, and with the resolution of our algorithm limited to $1/N$, independent of the SNR, we can notice a significant gap between the asymptotic CRLB and the two iterations of the estimator algorithm at very large SNRs.

4.4   Motivation for Optimization

In terms of power grids, where the SNR is assumed to be relatively high, using more samples than what is required for optimized performance is deemed unnecessary due to the estimator being biased at large SNRs, as shown in Fig.4.11.

One might argue that with the advent of modern technology, the computational load is not really a major area of concern. However, if we look at the complexity of modern electrical grids, and the imminent introduction of Smart Grids, where frequency and phase analysis will play a crucial role in assessing and controlling power quality, it would be beneficial to have a fast converging frequency estimation scheme at several points across the grid.

The use of small sensors, or micro-controllers to conduct analysis on the grid, embedding a frequency estimation program would at first require the concerned developers or engineers to understand the trade-off's relative to accuracy and computational load. The noise present, while making measurements, need close attention in order to evaluate frequency estimates with minimum variance at high speeds. The dichotomous search algorithm as presented in this paper, would suffice in real-time scenarios, if a perfect balance between sampling parameters, and ease of computation is established.

4.5   Response to Small Independent Frequency Changes

Ideally in conventional power networks, the operational frequency across each phase is held constant for obvious reasons.

Testing the sensitivity of a power system's overall operating frequency to a small variation of individual phase frequency, could be a testing scenario for our algorithm to see whether or not the formulation of the complex exponential is possible, and inspect the variation of overall system frequency due to these small independent changes.

Under balanced conditions and assuming all phases operate at f Hz, the α component of the output of the Clarke's Transformation differs from the β component by $\dfrac{\pi}{2}$, which simplifies the formulation of the complex exponential.

The introduction of a small change in frequency across any phase at any point in time, would in plain words, mean that the corresponding phase sinusoid would be propagating at a faster rate than the ones associated with the other phases. It would be interesting to see how our estimation algorithm would behave, in light of such phenomena, given that the purpose of utilizing the Clarke's Transform is to encode all possible frequency information within the complex sinusoid.

For testing and verification purposes, we introduce a small frequency change, Δf, across one phase of the system, while letting the remaining two phases operating at the set system frequency.

4.5.1   Response to Small Frequency Change in Phase 'a'

The frequency variation associated with phase 'a' of our system is denoted as, Δf_a, such that $f_a = f \pm \Delta f_a$ and its application to our sample of voltage signals would yield,

$$v_a(k) = V_a(k)\cos(2\pi f_a k\Delta T + \phi) \tag{4.3}$$

$$v_b(k) = V_b(k)\cos(2\pi f k\Delta T + \phi - \frac{2\pi}{3}) \tag{4.4}$$

$$v_c(k) = V_c(k)\cos(2\pi f k\Delta T + \phi + \frac{2\pi}{3}) \tag{4.5}$$

in which f is the fundamental frequency, $\phi = 0$ and the voltage amplitudes in each phase is set to unity.

$$\mathbf{v}_{\alpha\beta}(k) = \frac{2}{3}\begin{pmatrix} 1 & -\dfrac{1}{2} & -\dfrac{1}{2} \\ 0 & \dfrac{\sqrt{3}}{2} & -\dfrac{\sqrt{3}}{2} \end{pmatrix} \times \begin{pmatrix} \cos(2\pi f_a k\Delta T) \\ \cos(2\pi f k\Delta T - \dfrac{2\pi}{3}) \\ \cos(2\pi f k\Delta T + \dfrac{2\pi}{3}) \end{pmatrix} \tag{4.6}$$

This is now expanded and simplified to give us our α and β components.

$$v_\alpha(k) = \frac{2}{3}\left[\cos(2\pi k f_a \Delta T) - \frac{1}{2}\left(\cos(2\pi k f \Delta T - \frac{2\pi}{3}) + \cos(2\pi k f \Delta T + \frac{2\pi}{3})\right)\right] \tag{4.7}$$

or,

$$v_\alpha(k) = \frac{2\cos(2\pi k f_a \Delta T) + \cos(2\pi k f \Delta T)}{3} \tag{4.8}$$

The evaluation of $v_\beta(k)$ is as follows:

$$v_\beta(k) = \frac{2}{3} \times \frac{\sqrt{3}}{2}\left[\cos(2\pi f k \Delta T - \frac{2\pi}{3}) - \cos(2\pi f k \Delta T + \frac{2\pi}{3})\right] \tag{4.9}$$

or,

$$v_\beta(k) = \sin(2\pi k f \Delta T) \tag{4.10}$$

Variation in phase 'a' frequency			
f_a	f_b	f_c	Overall System Frequency Estimate
49	50	50	49.81
49.1	50	50	49.83
49.2	50	50	49.85
49.3	50	50	49.87
49.4	50	50	49.89
49.5	50	50	49.91
49.6	50	50	49.93
49.7	50	50	49.95
49.8	50	50	49.96
49.9	50	50	49.98
50.1	50	50	50.02
50.2	50	50	50.04
50.3	50	50	50.05
50.4	50	50	50.07
50.5	50	50	50.09
50.6	50	50	50.1
50.7	50	50	50.12
50.8	50	50	50.14
50.9	50	50	50.15
51	50	50	50.17

Table 4.1: Overall System Frequency Estimates with Respect to Independent Frequency Variation in Phase 'a'

4.5.2 Response to Small Frequency Change in Phase 'b'

Similar to the methods used to construct expressions for $v_\alpha(k)$ and $v_\beta(k)$ in case of a frequency deviation in phase 'a', we now form expressions for the $v_\alpha(k)$ and $v_\beta(k)$ terms in case of a small

frequency change in phase 'b'.

$$v_\alpha(k) = \frac{2}{3}\left[\cos(2\pi k f\Delta T) - \frac{1}{2}\left(\cos(2\pi f_b k\Delta T - \frac{2\pi}{3}) + \cos(2\pi f k\Delta T + \frac{2\pi}{3})\right)\right] \quad (4.11)$$

or,

$$v_\alpha(k) = \frac{2}{3}\left[\cos(2\pi k f\Delta T) - \left(\cos(\pi f_b k\Delta T + \pi k f\Delta T)\cos(\pi f_b k\Delta T - \pi k f\Delta T - \frac{2\pi}{3})\right)\right] \quad (4.12)$$

The expression of $v_\beta(k)$ is then given by,

$$v_\beta(k) = -\frac{2}{\sqrt{3}}\left[\sin(\pi f_b k\Delta T + \pi k f\Delta T)\sin(\pi f_b k\Delta T - \pi k f\Delta T) - \frac{2\pi}{3})\right] \quad (4.13)$$

Variation in phase 'b' frequency			
f_a	f_b	f_c	Overall System Frequency Estimate
50	49	50	49.86
50	49.1	50	49.87
50	49.2	50	49.88
50	49.3	50	49.9
50	49.4	50	49.91
50	49.5	50	49.93
50	49.6	50	49.94
50	49.7	50	49.95
50	49.8	50	49.97
50	49.9	50	49.98
50	50.1	50	50.02
50	50.2	50	50.03
50	50.3	50	50.05
50	50.4	50	50.06
50	50.5	50	50.08
50	50.6	50	50.1
50	50.7	50	50.11
50	50.8	50	50.13
50	50.9	50	50.15
50	51	50	50.16

Table 4.2: Overall System Frequency Estimates with Respect to Independent Frequency Variation in Phase 'b'

4.5.3 Response to Small Frequency Change in Phase 'c'

The expressions for the $v_\alpha(k)$ and $v_\beta(k)$ terms in this particular scenario is given by:

$$v_\alpha(k) = \frac{2}{3}\left[\cos(2\pi kf\Delta T) - \left(\cos(\pi fk\Delta T + \pi kf_c\Delta T)\cos(\pi fk\Delta T - \pi kf_c\Delta T - \frac{2\pi}{3})\right)\right] \quad (4.14)$$

$$v_\beta(k) = -\frac{2}{\sqrt{3}}\left[\sin(\pi fk\Delta T + \pi kf_c\Delta T)\sin(\pi fk\Delta T - \pi kf_c\Delta T) - \frac{2\pi}{3})\right] \quad (4.15)$$

Variation in phase 'c' frequency			
f_a	f_b	f_c	Overall System Frequency Estimate
50	50	49	49.34
50	50	49.1	49.4
50	50	49.2	49.47
50	50	49.3	49.53
50	50	49.4	49.6
50	50	49.5	49.67
50	50	49.6	49.73
50	50	49.7	49.8
50	50	49.8	49.87
50	50	49.9	49.93
50	50	50	50
50	50	50.1	50.07
50	50	50.2	50.13
50	50	50.3	50.2
50	50	50.4	50.27
50	50	50.5	50.33
50	50	50.6	50.4
50	50	50.7	50.47
50	50	50.8	50.53
50	50	50.9	50.6
50	50	51	50.67

Table 4.3: Overall System Frequency Estimates with Respect to Independent Frequency Variation in Phase 'c'

Chapter 5

Conclusion

The need for a frequency estimation algorithm for three-phase power systems has been acknowledged. An extensive research has been conducted on various methodologies developed by researchers in the past and their supporting literature has been reviewed to understand the basic concepts and requirements for an accurate and fast converging estimator of power frequency.

Upon reviewing some common techniques in tracking power system frequency, a strong motivation has been developed to propose and subsequently implement a new method to be used in real-time scenarios. The Clarke's transformation is a powerful tool that has been proven to significantly reduce the complexities involved in analysing the frequency contained within three-phase power signals, by resolving the three phase voltages into a single complex exponential which has a more physically meaningful and robust representation for single phase estimator algorithms to be carried out.

As a result, a few novel single phase estimators designed for complex sinusoids have also been investigated and their supporting literature have been heavily analysed. This paper is dedicated to promote a novel technique of three-phase frequency estimation that is reliable in terms of accuracy and speed of convergence. In contrast to the current methodologies, some of which have been reviewed in this paper, our estimator demonstrates great resilience while heavily reducing the speed of computation while catering towards the presence of noise and its effects. A few key design constraints have also been addressed in order to establish a level field between computational speed(or load) and accuracy of results, and its safe to say our estimator, in addition to being unbiased, meets all the basic requirements.

5.1   Future Work

- First and foremost, as seen throughout the paper, arbitrary signals have been used to assess the estimation algorithm's performance, and it is only realistic to extend its operation onto three-phase voltage signals sampled, in real-time, from real "points" across the power network.

- Introduction of voltage or current harmonics across numerous points on the network, due to a variety of reasons, needs closer attention, and our frequency estimator could be deployed to analyse overall network health under these circumstances.

- The frequency estimates derived via our methodology can be used to estimate the phase at different points on the grid, where it varies continuously due to the application of the various types of loads. Hence, power quality control and protection mechanisms can be easily implemented drawing on from our estimator's operational characteristics.

- In this paper, we have assumed balanced, sinusoidal conditions. Ideally, we would want to assume the unbalanced voltage and current conditions, and make necessary changes to our solution in order to provide more robustness towards various types of scenarios.

- Smart Grids, being labelled as the future of electricity grids, would require frequency and/or subsequent phase estimation across numerous points on the network, for network diagnostic and assessment purposes. This would require the use of highly efficient sensors to ensure constant monitoring of our power parameters. It would be interesting to see if our estimation scheme would be implementable on a micro-controller level, and address all the major design constraints and "fine-tune" the procedures for fast, reliable and efficient frequency tracking.

Appendix A

Circularity of Complex Exponential under Unbalanced Three-Phase Conditions

For a three-phase system, the complex valued $v(k) = v_\alpha(k) + jv_\beta k$ comprises the standard part (left-hand term) and the conjugate part (right hand term). That is,

$$v(k) = A(k)e^{j(2\pi f + \phi)} + B(k)e^{-j(2\pi f + \phi)} \tag{A.1}$$

where,

$$A(k) = \frac{\sqrt{6}(v_a(k) + v_b(k) + v_c(k))}{6} \tag{A.2}$$

$$B(k) = \frac{\sqrt{6}(2v_a(k) - v_b(k) - v_c(k))}{12} - j\frac{\sqrt{2}(v_b(k) - v_c(k))}{4} \tag{A.3}$$
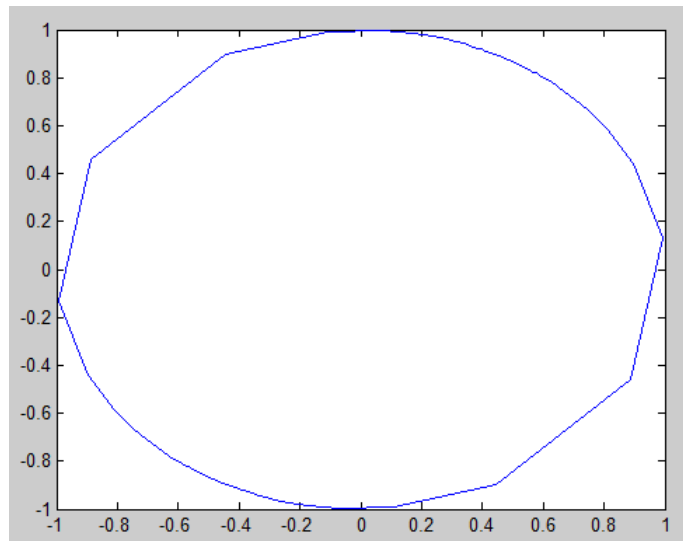

Figure A.1: Non-circularity of complex exponential under unbalanced conditions

The complex sinusoid, $v(k)$ has the form as shown in Figure A.1 due to $B(k) \neq 0$ under unbalanced conditions.

Bibliography

[1] Electrical systems. [Online]. Available: http://wikitravel.org/en/Electrical_systems

[2] Power quality. [Online]. Available: http://en.wikipedia.org/wiki/Power_quality# mediaviewer/File:Variation_of_utility_frequency.svg

[3] E. Aboutanios, "Estimating the parameters of sinusoids and decaying sinusoids in noise," *IEEE Instrumentation and Measurement Magazine*, 2011.

[4] J. J. T. Miodrag D. Kusljevic and L. D. Jovanovic, "Frequency estimation of three-phase power system using weighted-least-square algorithm and adaptive fir filtering," *IEEE Transactions on Instumentation and Measurement*, vol. 59, no. 2, pp. 322–329, February 2010.

[5] R. Wettimuny, "Power system frequency and time deviation monitoring report – reference guide," Electricity System Operations Planning and Performance, Australian Energy Market Operator (AEMO), Tech. Rep. 2, 2 July 2012.

[6] M. H. Bollen, "Voltage sags in three-phase systems," *IEEE Power Eng. Rev.*, vol. 21, no. 9, pp. 8–15, 2001.

[7] S. S. M. F. M. P. A. C. M. V. R. Math H.J. Bollen, Irene Y.H. Gu and P. F. Ribeiro, "Bridging the gap between signal and power," *IEEE Signal Processing Magazine*, vol. 26, no. 7, pp. 11–31, 2009.

[8] H. L. Zhu Chen, Zafer Sahinoglu, "Fast frequency and phase estimation in three phase power systems," *Mitsubishi Electric Research Laboratories TR2013-052*, 2013 2013.

[9] D. H. Dini and D. P. Mandic, "Widely linear modelling for frequency estimation in unbalanced three-phase power systems," *IEEE Transactions on Instumentation and Measurement*, vol. 62, no. 2, pp. 353–363, February 2013.

[10] Y. Liao, "Phase and frequency estimation: High-accuracy and low-complexity techniques," Master's thesis, WORCESTER POLYTECHNIC INSTITUTE, 2011.

[11] O. Vainio and S. Ovaska, "Digital filtering for robust 50/60 hz zero-crossing detectors," *IEEE Transactions on Instumentation and Measurement*, vol. 45, no. 2, pp. 426–430, April 1996.

[12] D. Rife and R. Boorstyn, "Single tone parameter estimation from discrete-time observations," *IEEE Trans.Inf.Theo.*, vol. 20, pp. 591–598, September 1974.

[13] E. Aboutanios and B. Mulgrew, "Iterative frequency estimation by interpolation on fourier coefficients," *IEEE Transactions on Signal Processing*, vol. 53, no. 4, pp. 1237–1242, April 2005.

[14] E. Aboutanios, "Estimation of the frequency and decay factor of a decaying exponential in noise," *IEEE Trans. Sig. Process*, vol. 58, pp. 501–509, February 2010.

[15] B. Quinn and E. Hannan, *The Estimation and Tracking of Frequency.* New York: Cambridge University Press, 2011.

[16] M. Kusljevic, "A simple recursive algorithm for frequency estimation," *IEEE Transactions on Instumentation and Measurement*, vol. 53, no. 2, pp. 335–340, April 2004.

[17] M. D. Kusljevic, "A simple method for design of adaptive filters for sinusoidal signals," *IEEE Transactions on Instumentation and Measurement*, vol. 57, no. 10, pp. 2242–2249, October 2008.

[18] C. Y. J.Z. Yang and C. Liu, "A new method for power signal harmonic analysis," *IEEE Transactions on Power Delivery*, vol. 20, no. 2, pp. 1235–1239, April 2005.

[19] S. Chung, "A phase tracking system for three phase utility interface inverters," *IEEE Transactions on Power Delivery*, vol. 15, no. 3, pp. 431–438, May 2000.

[20] B. Boashash, "Estimating and interpreting the instantaneous frequency of a signal: Part i: Fundamentals, part ii: Algorithms and applications," *Proc. IEEE*, vol. 80, pp. 520–568, April 1992.

[21] T. Lobos and J. Rezmer, "Real-time determination of power system frequency," *IEEE Transactions on Instumentation and Measurement*, vol. 46, no. 4, pp. 877–881, August 1997.

[22] E. Clarke, *Circuit Analysis of a.c. Power Systems.* New York: Wiley, 1943, vol. I.

[23] M. Akke, "Frequency estimation by demodulation of two complex signals," *IEEE Trans. Power Delivery*, vol. 12, no. 1, pp. 157–163, 1997.